Simulation Studies of Various Converter Techniques to DFIG Based WECS

K. H. Phani Shree*
Assistant Professor,
Dept of EEE, JNTUH,
College of Engineering Hyderbad,

Dr. S. V. Jaya Ram Kumar
Professor,
Dept of EEE, JNTUH,
College of Engineering Hyderbad,

ABSTRACT.

DFIG (Doubly fed induction generator) based wind farms are gaining popularity because of inherent advantages of DFIG like independent control of active and reactive powers, lower converter ratings, variable speed operation. Rotor side converter is used to control stator fed active reactive powers independently into the grid by implementing vector control technique. So in this paper various converter topologies have been implemented for RSC and performance is analyzed and total harmonic distortion is compared. The comparative study demonstrates the capability of SVPWM technique in obtaining good dynamic response with lowest total harmonic distortion. ***KEYWORDS: DFIG, converters, SVPWM,***

Multilevel converter.

1. INTRODUCTION

Wind energy system is recently getting lot of attention, because they are cost competitive, environmental clean and safe renewable power sources, as compared fossil fuel and nuclear power generation.

The utilization of wind turbine to produce electricity is increasing rapidly in different parts of the world. It has become one of the main alternatives for non pollutant and environmentally friendly type for power generation.

Doubly fed induction generator (DFIG) is one of the most popular generator because of availability of slip rings. The power electronic equipment used in DFIG has to handle only a fraction (20–30%) of the total system power.

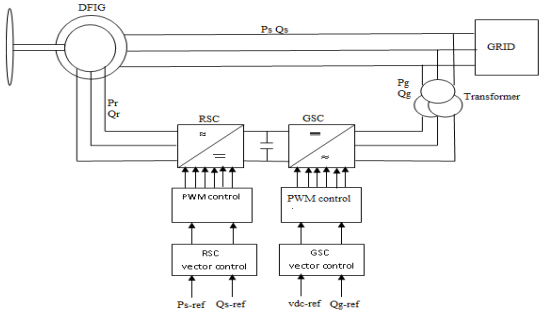

Fig.1 DFIG based WECS

2. WIND TURBINE

The power extracted from the air stream by the turbine blades can be characterized by Equation

$$P_t = \frac{1}{2}\rho A V^3 C_p(\lambda, \beta) \quad (1)$$

Where

ρ - air density (kgm-3)

V - wind speed (ms-1)

A -Turbine swept area (m^2)

β - Blade pitch angle (deg)

λ - Tip speed ratio

Cp itself is not a constant for a given airfoil, but rather is dependent on tip-speed ratio (λ), which is the ratio of the speed of the tip of the blade to the speed of the moving air stream and blade pitch angle (β), here pitch angle is usually around zero when the wind speed is below rated speed.

3. MODELLING OF DFIG

Modeling is very useful for studying the transient and dynamic behavior of any electrical machines and of interconnected electrical machine system. Using the Concordia and Park transformation allows writing a dynamic model in a d-q reference frame from the traditional a-b-c frame as follows [7].

Stator voltages and rotor voltages

$$V_{ds} = R_s i_{ds} - \omega_e \emptyset_{qs} + p\emptyset_{ds} \quad (2)$$

$$V_{qs} = R_s i_{qs} + \omega_e \emptyset_{ds} + p\emptyset_{qs} \quad (3)$$

$$V_{dr} = R_r i_{dr} - (\omega_e - \omega_r)\emptyset_{qr} + p\emptyset_{dr} \quad (4)$$

$$V_{qr} = R_r i_{qr} + (\omega_e - \omega_r)\emptyset_{dr} + p\emptyset_{qr} \quad (5)$$

The stator and rotor flux are

$$\emptyset_{ds} = L_s i_{ds} + L_m i_{dr} \quad (6)$$

$$\emptyset_{Qs} = L_s i_{qs} + L_m i_{qr} \quad (7)$$

$$\emptyset_{qr} = L_r i_{qr} + L_m i_{qs} \quad (8)$$

$$\emptyset_{dr} = L_r i_{dr} + L_m i_{ds} \quad (9)$$

Electromagnetic torque

$$T_e = -\left(\frac{3}{2}\right)\left(\frac{P}{2}\right)\left[\emptyset_{qs} i_{ds} - \emptyset_{ds} i_{qs}\right] \quad (10)$$

The motion of the generator is

$$\frac{d\omega_r}{dt} = (T_e - T_l)\left(\frac{1}{J}\right)\left(\frac{2}{P}\right) \quad (11)$$

Active and reactive powers of stator

$$Ps = \frac{3}{2}\left(V_{ds} i_{ds} + V_{qs} i_{qs}\right)$$
$$Q_s = \frac{3}{2}\left(V_{qs} i_{ds} - V_{ds} i_{qs}\right) \quad (12)$$

3. CONTROL STRATEGIES:

3.1 RSC control

Stator flux orientation technique is used to get the decoupled control of active and reactive powers, i.e. $\emptyset_s = \emptyset_{ds}$, $\emptyset_{qs} = 0$.

$$i_{ds} = \frac{\emptyset_s}{L_s} - \frac{L_m}{L_s} i_{dr}\ , \qquad i_{qs} = -\frac{L_m}{L_s} i_{qr}$$

$$V_{qr_{ref}} = V_{qr}^1 + L_r \sigma i_{dr}(\omega_e - \omega_r)$$

$$+\frac{L_m}{L_s}\emptyset_{ds}(\omega_e-\omega_r) \quad (13)$$

$$V_{dr\_ref} = V_{dr}^1 + L_r\sigma i_{qr}(\omega_e-\omega_r) \quad (14)$$

Where $\sigma = \left(1-\frac{L_m^2}{L_sL_r}\right)$

The active and reactive power becomes

$$P_s = -\left(\frac{3}{2}\right)\left(\frac{L_m}{L_s}\right)V_s i_{qr}\ , \quad (15)$$

$$Q_s = -\left(\frac{3}{2}\right)V_s\left[\frac{\emptyset_s}{L_s}-\frac{L_m}{L_s}i_{dr}\right] \quad (16)$$

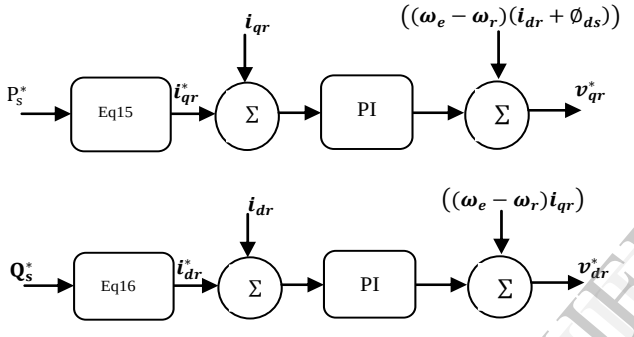

3.2 GSC Control

Stator flux orientation technique is used to get the decoupled control of active and reactive powers, i.e. $\emptyset_s = \emptyset_{ds}$, $\emptyset_{qs} = 0$.

$$i_{gd\_ref} = \frac{2}{3}\frac{Q_{q\_ref}}{v_{gq}} \quad (17)$$

$$V_{gd\_ref} = -V_{gd}' + \omega_e L_g i_{gq} + V_{gd} \quad (18)$$

$$V_{gq\_ref} = -V_{gq}' - \omega_e L_g i_{gd} \quad (19)$$

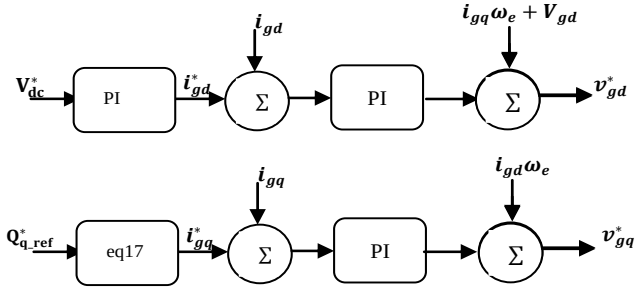

4. CONVERTER TOPOLOGIES

In DFIG configuration two back to back connected converters are used. One is Rotor side converter (RSC) and another is grid side converter (GSC) as shown below. In sub synchronous operation RSC acts as inverter and GSC acts as rectifier. In case of super synchronous mode action of these converters changes vice versa.

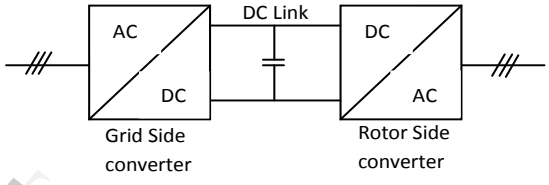

Fig.2. converter topology

SINUSOIDAL PWM CONVERTERS

In DFIG model the output of the rotor slip power is fed to the grid through back to back connected PWM converters through a common DC link. Rotor side converter acts as a PWM rectifier and grid side converter acts as PWM inverter during the machine working in sub synchronous mode. PWM rectifier is used to convert the variable magnitude, variable frequency voltage at the induction generator rotor terminals to DC voltage. DC link capacitor acts as a stiff voltage source and it provides dc isolation between the two converters.Fig.4 depicts the two back-to-back connected PWM converters.

PWM VOLTAGE SOURCE INVERTER MODEL

The DC power available at the rectifier output is filtered and converted to AC power using a PWM inverter employing sinusoidal modulation.

In case of PWM converters balanced three phase voltages are developed as reference voltages and they are compared with carrier signals. In all the simulations carrier frequency has been considered as 3000Hz.

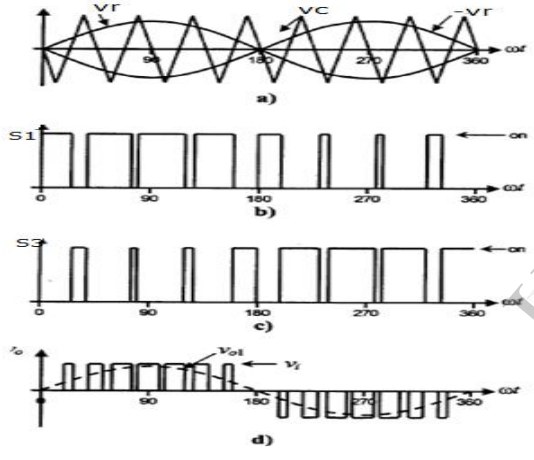

Fig.3.sinusoidal pulse width modulation waveforms a) sinusoidal and triangular signals b) switch S1 state c) switch S3 state d) ac output voltage

3.2 MULTI LEVEL CONVERTERS

It is easy to produce a high-power, high-voltage with the multilevel structure because of the way in which device voltage stresses are controlled in the structure. Increasing the number of voltage levels in the inverter without requiring higher ratings on individual devices can increase the power rating. The unique structure of multilevel voltage source inverters allows them to reach high voltages with low harmonics without the use of transformers or series-connected synchronized switching devices. As the number of voltage levels increases, the harmonic content of output voltage and current decreases significantly.

For The *m*-level multilevel inverters to get the required *m* levels in output the number of capacitors needed is (*m*−1), voltage across each capacitor is defined as $V_{DC}/(m-1)$. The required no of clamping devices and switching devices are (*m*-1)x(*m*-2) and 2x(*m*-1) per phase respectively. DFIG model has been developed considering RSC as multilevel converter.

3.3 SPACE VECTOR MODULATION PWM

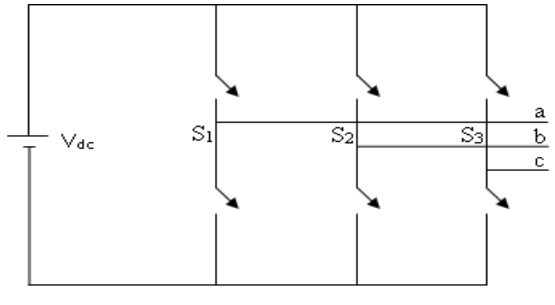

Fig 4.three phase inverter

From fig 4 three phase inverter each leg switches are defined as S1,S2 and S3.if S_k(k=1,2,3) is 1 upper switch is ON

otherwise lower switch is ON i.e. S_k is 0. There are eight configurations possible with these three phase legs. Out of eight, in two combinations all the upper switches or all the lower switches of each pole are simultaneously ON result in zero output voltage from the inverter. These two combinations are referred as **null states** of

the inverter. The remaining six switching combinations, wherein either two of the high side (upper) switches and one of the low side (lower) switch conduct, or vice-versa, are **active states.** The eight vectors are called the basic space vectors and are denoted by V_0, V_1, V_2, V_3, V_4, V_5, V_6, and V_7. V_0 and V_7 are null state vectors.

The eight space vectors are represented in fig 5 along with ON/OFF of states of poles S1, S2 and S3.

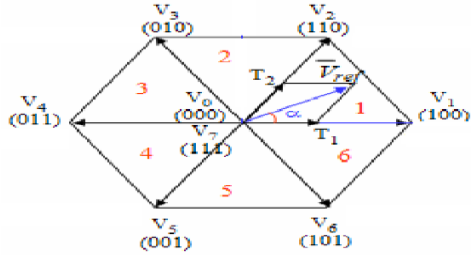

fig 5. Basic switching vectors and sectors

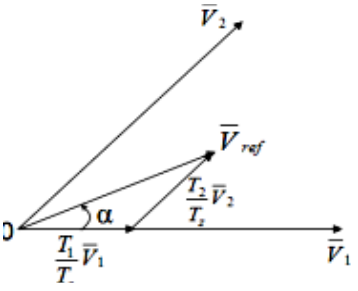

fig 6. Reference vector as a combination of adiacent vectors at sector 1

Switching time duration at Sector 1

From fig.6 the switching time durations can be calculated as follows

In fig 6. α is the angle made by reference voltage vector $\bar{V}_{ref}$ with voltage vector $\bar{V}_1$

$$\int_0^{T_z} \bar{V}_{ref} = \int_0^{T_1} \bar{V}_1\, dt + \int_{T_1}^{T_1+T_2} \bar{V}_2\, dt + \int_{T_1+T_2}^{T_z} \bar{V}_0\, dt$$

$$T_Z \bar{V}_{ref} = (T_1 \bar{V}_1 + T_2 \bar{V}_2)$$

$$T_z \cdot |\bar{V}_{ref}| \cdot \begin{bmatrix}\cos\alpha \\ \sin\alpha\end{bmatrix} = T_1 \cdot \frac{2}{3} \cdot V_{dc} \begin{bmatrix}1 \\ 0\end{bmatrix}$$

$$+T_2 \cdot \frac{2}{3} \cdot V_{dc} \begin{bmatrix}\cos(\pi/3) \\ \sin(\pi/3)\end{bmatrix}$$

(Where, $0 \leq \alpha \leq 60^0$)

$$\therefore\ T_1 = T_z \cdot a \cdot \frac{\sin(\pi/3 - \alpha)}{\sin(\pi/3)}$$

$$\therefore\ T_2 = T_z \cdot a \cdot \frac{\sin(\alpha)}{\sin(\pi/3)}$$

$$\therefore T_0 = T_z - (T_1 + T_2) \begin{bmatrix}\text{where}, T_z = \frac{1}{f_z} \text{ and} \\ a = \frac{|\bar{V}_{ref}|}{\frac{2}{3}V_{dc}}\end{bmatrix}$$

- Switching time duration at any Sector

$$T_1 = \frac{\sqrt{3} \cdot T_z \cdot |\bar{V}_{ref}|}{V_{dc}} \left[sin\left(\frac{n}{3}\pi - \alpha\right)\right]$$

$$T_2 = \frac{\sqrt{3} \cdot T_z \cdot |\bar{V}_{ref}|}{V_{dc}} \left[sin\left(\alpha - \frac{n-1}{3}\pi\right)\right]$$

[Where, n=1,2...6(i.e.,Sector1 to 6), $0 \leq \alpha \leq 60^0$]

$$T_0 = T_z - (T_1 + T_2)$$

Table 1. Switching patterns

Sector	Upper switches	Lower switches
1 (V_{100}-V_{110})	S_1 $T_1+T_2+T_0/2$ S_3 $T_2+T_0/2$ S_5 $T_0/2$	S_4 $T_0/2$ S_6 $T_1+T_0/2$ S_2 $T_1+T_2+T_0/2$
2 (V_{110}-V_{010})	S_1 $T_1+T_0/2$ S_3 $T_1+T_2+T_0/2$ S_5 $T_0/2$	S_4 $T_2+T_0/2$ S_6 $T_0/2$ S_2 $T_1+T_2+T_0/2$
3 (V_{010}-V_{011})	S_1 $T_0/2$ S_3 $T_1+T_2+T_0/2$ S_5 $T_2+T_0/2$	S_4 $T_1+T_2+T_0/2$ S_6 $T_0/2$ S_2 $T_1+T_0/2$
4 (V_{011}-V_{001})	S_1 $T_0/2$ S_3 $T_1+T_0/2$ S_5 $T_1+T_2+T_0/2$	S_4 $T_1+T_2+T_0/2$ S_6 $T_2+T_0/2$ S_2 $T_0/2$
5 (V_{001}-V_{101})	S_1 $T_2+T_0/2$ S_3 $T_0/2$ S_5 $T_1+T_2+T_0/2$	S_4 $T_1+T_0/2$ S_6 $T_1+T_2+T_0/2$ S_2 $T_0/2$
6 (V_{101}-V_{100})	S_1 $T_1+T_2+T_0/2$ S_3 $T_0/2$ S_5 $T_1+T_0/2$	S_4 $T_0/2$ S_6 $T_1+T_2+T_0/2$ S_2 $T_2+T_0/2$

6. SIMULATION RESULTS

To investigate the effectiveness of the converter technologies, numerical simulation was carried out on a typical grid-connected wind energy conversion system as shown in Fig. 1. The system parameters are mentioned in the appendix. In the simulation, a number of disturbances are considered at various time instants to test the system. At t=2 sec, step change in the active power set point, at t=3 sec, step change in the reactive power set point and at t=4sec step change in the output mechanical power have been considered in all the configurations.

At t=2 sec a step change in the DFIG's output active power from -1000W to -2000W is set. The reactive power reference up to t=3 sec is set at zero and at t=3 sec a step change of 500VARS has been simulated. The wind mechanical power fed to the rotor shaft is changed from 12m/s to 13 m/s at t=4 sec. These scenarios can simulate the disturbance in the maximum power point tracking. The responses of the generator torque, speed, stator currents, rotor current, rotor phase voltage, stator active, reactive powers have been presented.

It is shown in Figs. 6.1, 6.2, 6.3, 6.4, and 6.5. The controller tracks the reference of the output active power very quickly; When the DFIG's active power set point has a step change. As the active power reference changes, the DFIG's output reactive power also undergoes a small oscillation. From equations (15) & (16), we can see that the reactive power

and active power are related to *idr* and *iqr* respectively, so the changes in active power and reactive power are realized by the changes in i_{qr} and i_{dr}. from the Figs. 6.1(h), 6.1(i) and 6.1(f), 6.1(e) match this prediction very well. The first two figures show the electromagnetic torque and the rotor speed. Initially, the stator active power set point is higher than the input mechanical power, so the rotor speed is lower than the synchronous speed, the electromagnetic torque will increase consequently.

At t=3 reactive power change is simulated. The stator reactive power reference is zero before 3 sec and changes to 500Var at 3s. The responses of the generator variables to the step change in the reactive power reference are shown in Fig. 6.1.

As the reactive power set point steps up at 3s, the rotor *d*-axis current *idr* changes. This is consistent with that the reactive power is more related to *idr*, the electromagnetic torque, active power and speed will not get effected.

At t=4 s there is a step change in the input wind mechanical power. The stator output active power set point and reactive power set point are -2000W and 500Vars respectively. The input wind speed changes from 12m/s to 13m/s. The responses of the generator variables to the step change in the input wind mechanical power are shown in Fig.6.1.As the input power is more than the output power of stator DFIG accelerates and speed increases. . The rotor-side converter is injecting power to the DFIG. When a step change in the input mechanical power occurs, since the set points of stator output active power and reactive power remain unchanged, the output active or reactive power from the stator does not change.

6.1 DFIG WITH SPWM CONVERTER

In this configuration RSC and GSC have been simulated as sinusoidal PWMs. The response of DFIG with wind turbine is as follows. In this configuration converters are controlled by SPWM technique.

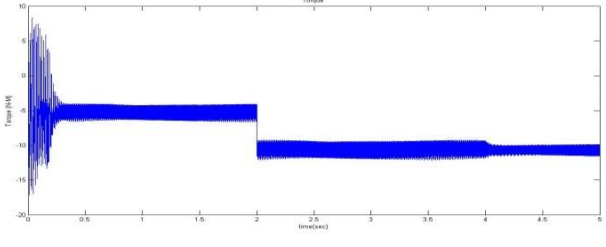

Fig 6.1 (a) Torque

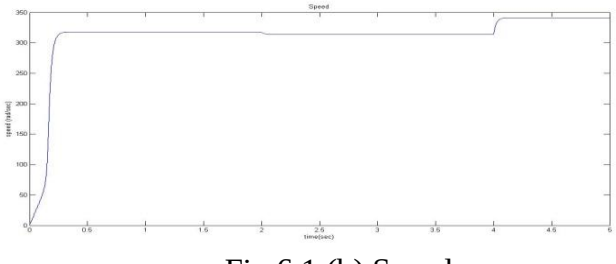

Fig 6.1 (b) Speed

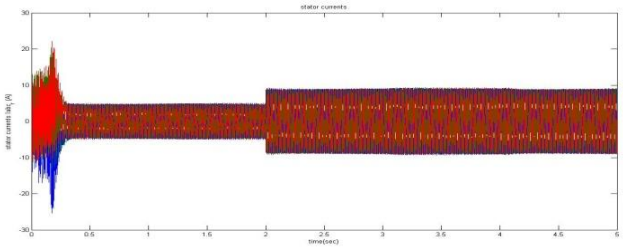

Fig 6.1 (c) Stator currents

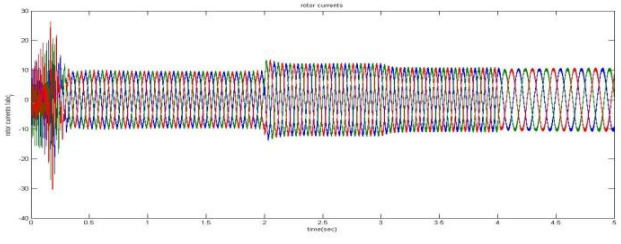

Fig 6.1 (d) Rotor currents

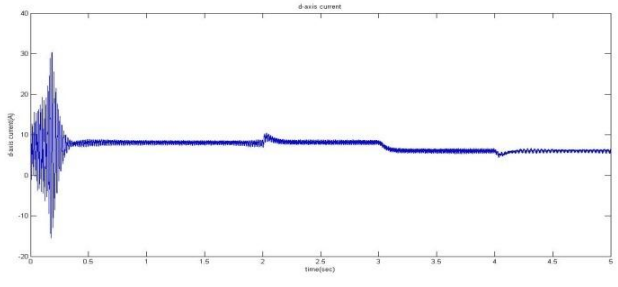

Fig 6.1 (e) rotor d-axis current

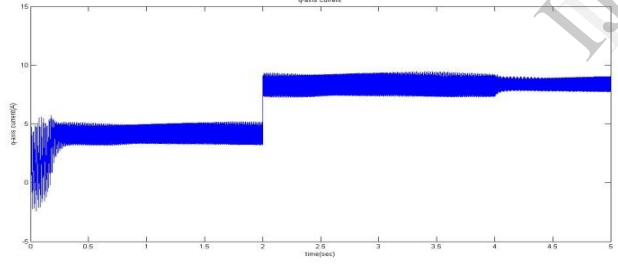

Fig 6.1 (f) rotor q-axis current

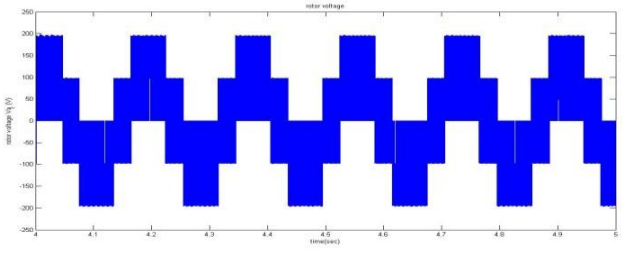

Fig 6.1 (g) Rotor Phase voltage

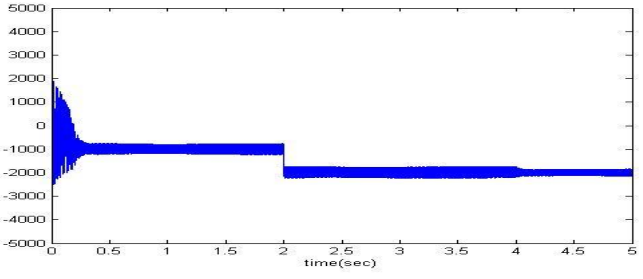

Fig 6.1 (h) Active Power

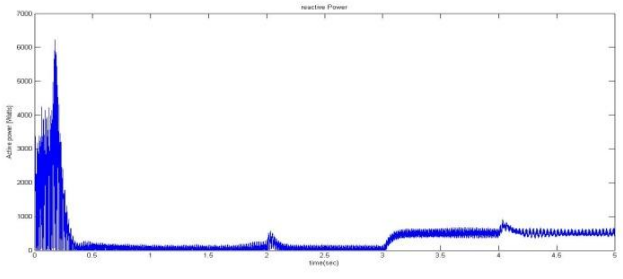

Fig 6.1 (i) Reactive Power

6.2 DFIG WITH CASCADED SPWM CONVERTER:

In this configuration two SPWM inverters have been cascaded to realize RSC. The response of DFIG is as follows.

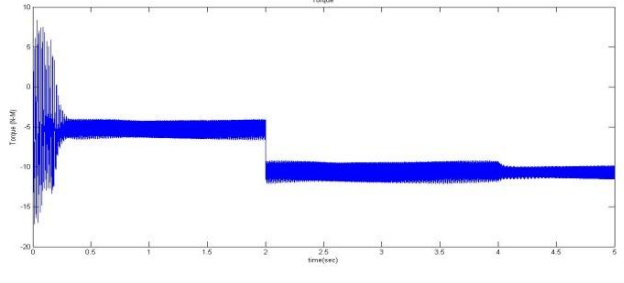

Fig 6.2 (a) Torque

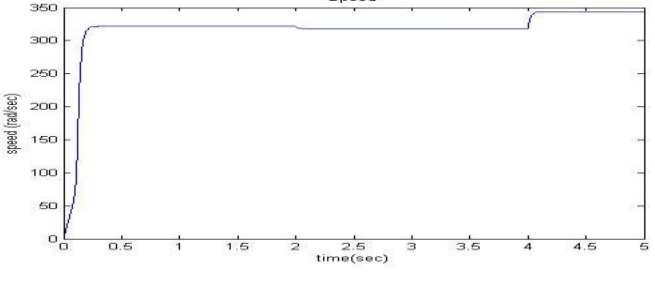

Fig 6.2 (b) Speed

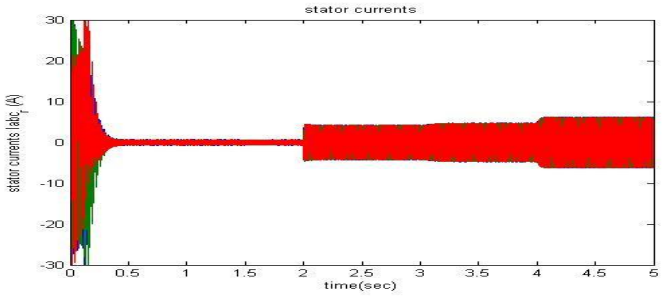

Fig 6.2 (c) Stator currents

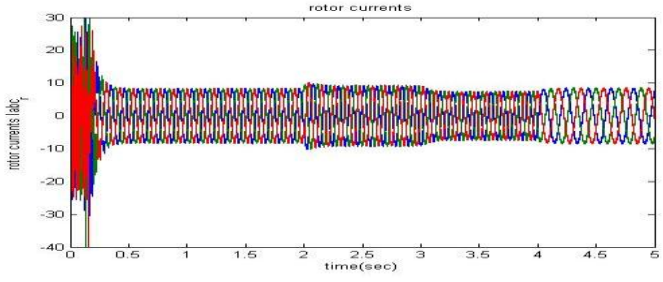

Fig 6.2 (d) Rotor currents

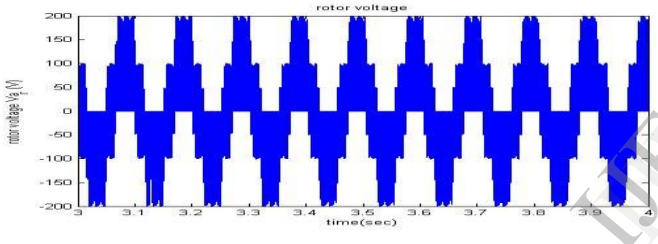

Fig 6.1 (e) Rotor Phase voltage

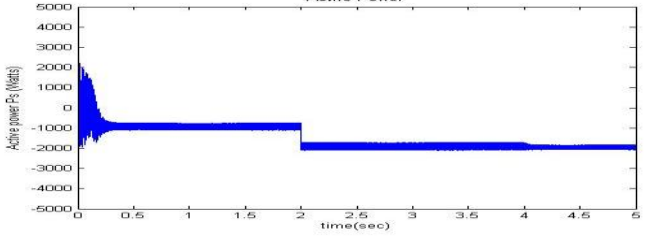

Fig 6.1 (f) Active Power

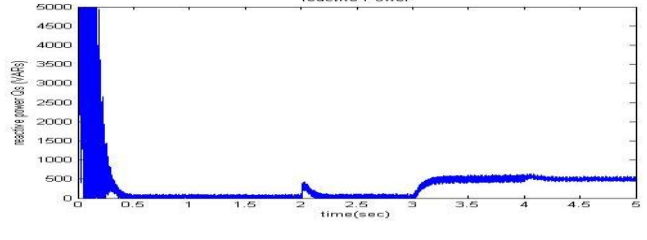

Fig 6.2 (g) Reactive Power

6.3 DFIG WITH MULTILEVEL (3-LEVEL) CONVERTER:

In this configuration RSC has been realized as three level multilevel inverter. So from the rotor voltage waveform three obvious changes can be observed. The decoupled response using multilevel converter is achieved. The rating of converter has been reduced using multilevel configurations.

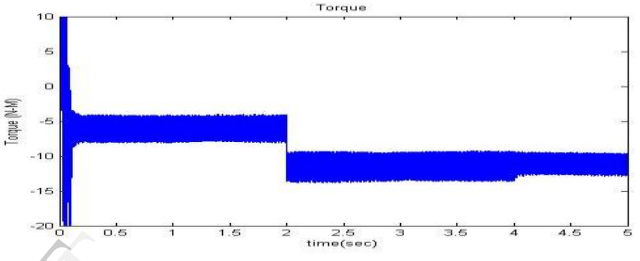

Fig 6.3 (a) Torque

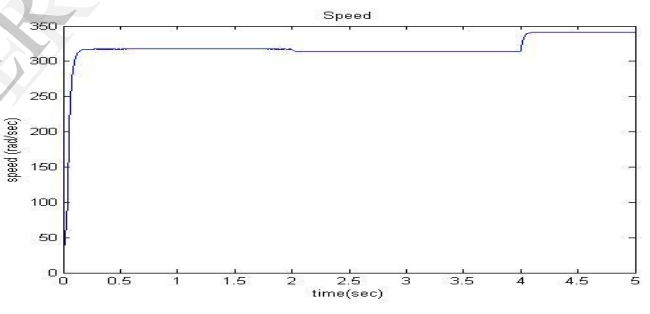

Fig 6.3 (b) Speed

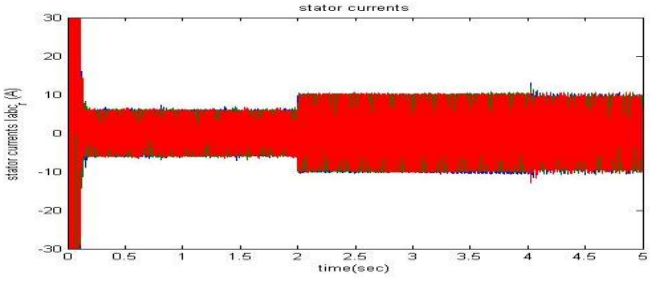

Fig 6.3 (c) Stator currents

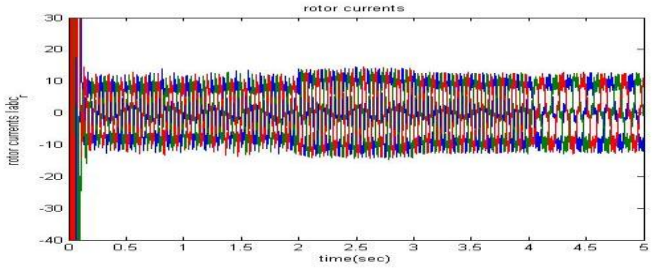

Fig 6.3 (d) Rotor currents

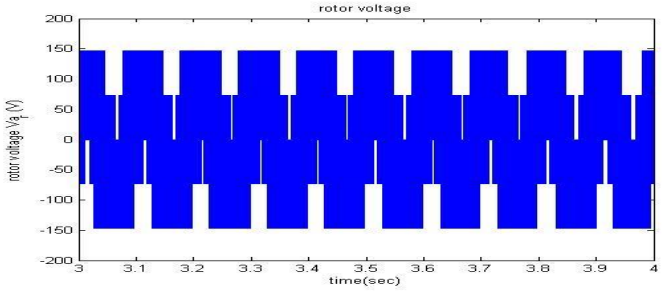

Fig 6.3 (e) Rotor Phase voltage

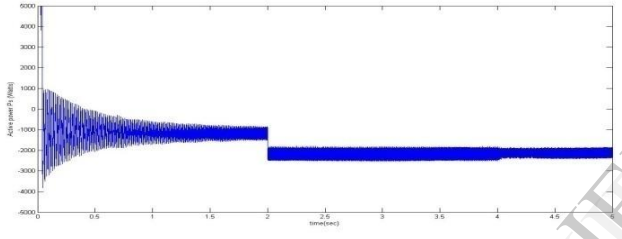

Fig 6.3 (f) Active Power

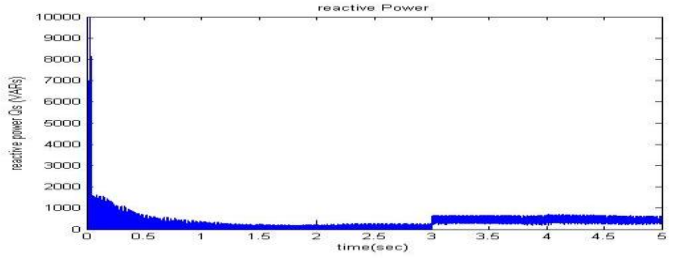

Fig 6.2 (g) Reactive Power

6.4 DFIG WITH MULTI LEVEL (5-LEVEL) CONVERTER

In this configuration RSC has been designed as 5-Level converter. This can be observer by seeing rotor phase voltage waveform. The following results shows the response of DFIG based WECS. In this configuration also set points of active, reactive and mechanical input powers have been tracked effectively. The ratings of the converter have been reduced further when 5-levelconverter is simulated.

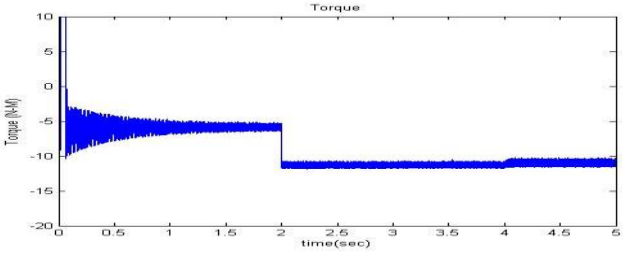

Fig 6.4 (a) Torque

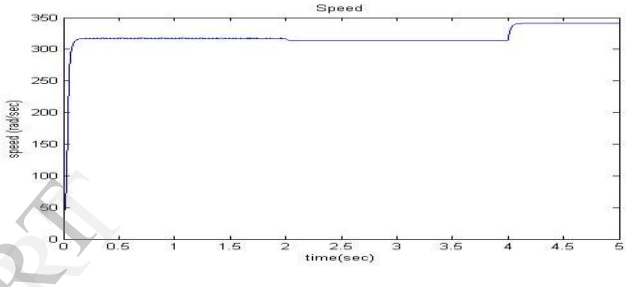

Fig 6.4 (b) Speed

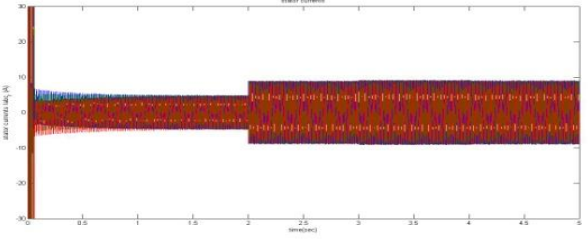

Fig 6.4 (c) Stator currents

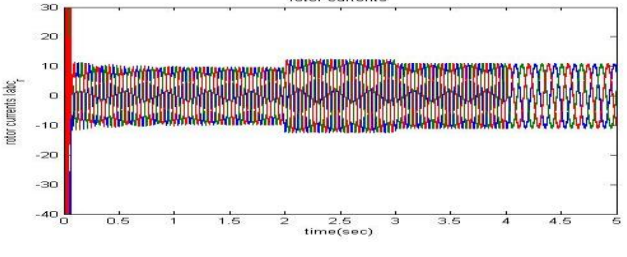

Fig 6.4 (d) Rotor currents

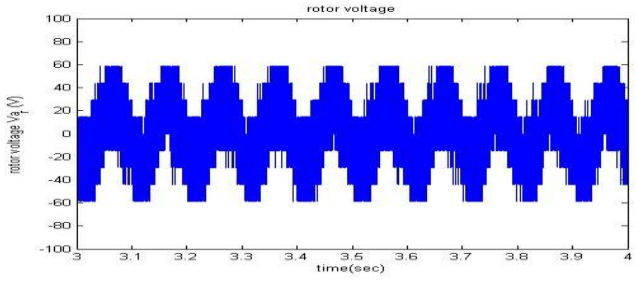

Fig 6.4 (e) Rotor Phase voltage

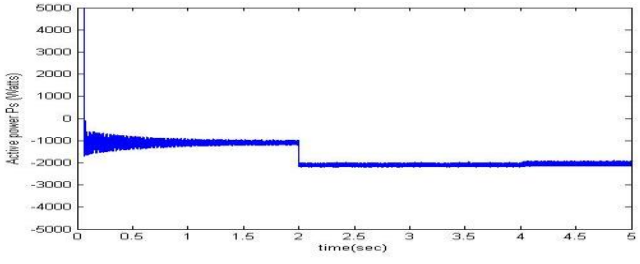

Fig 6.4 (f) Active Power

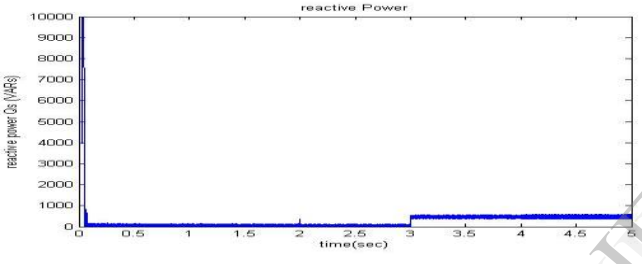

Fig 6.4 (g) Reactive Power

6.5 DFIG WITH SPACE VECTOR PWM CONVERTER

In this configuration RSC has been modeled as Space vector PWM converter. The following result shows the response of DFIG based WECS. In this configuration also set points of active, reactive and mechanical input powers have been tracked effectively.

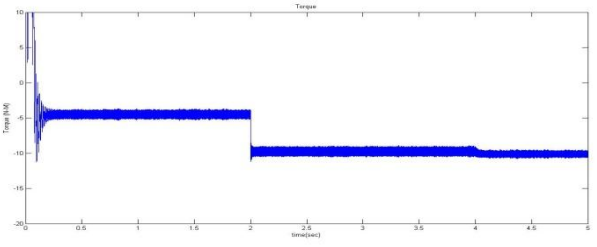

Fig 6.5 (a) Torque

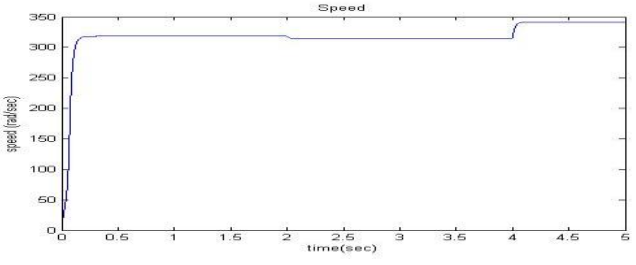

Fig 6.5 (b) Speed

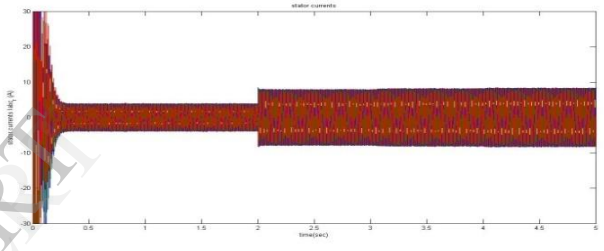

Fig 6.5 (c) Stator currents

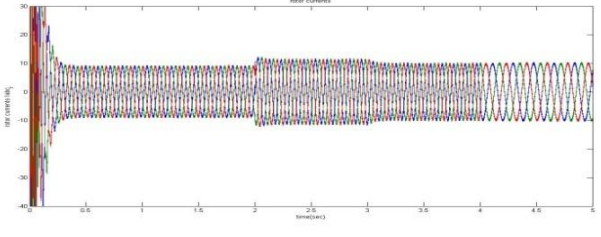

Fig 6.5 (d) Rotor currents

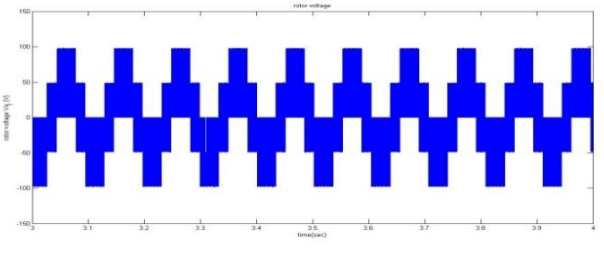

Fig 6.5 (e) Rotor Phase voltage

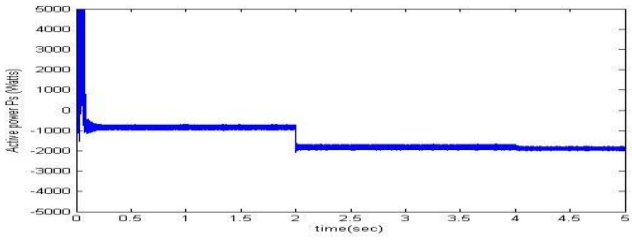

Fig 6.5 (f) Active Power

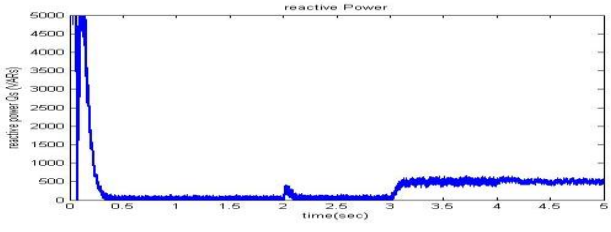

Fig 6.5 (g) Reactive Power

Total harmonic distortions have been compared in various topologies of DFIG.

Table 2. Harmonic analysis of DFIG

DFIG with different converters	Stator currents	Rotor currents
SPWM converter	3.21	3.22
Cascaded SPWM converter	4.90	2.44
3-level multilevel converter	4.72	5.00
5-level multilevel converter	2.65	2.13
Space Vector PWM converter	2.44	2.17

From the table 2 it can be seen that 5-level multilevel converter and Space vector PWM converters are giving less total harmonic distortion.

CONCLUSIONS

This paper investigates on dynamic modeling of DFIG based WECS. Various converter topologies have been developed for RSC of DFIG using MATLAB/Simulink software. SVPWM produces more dc voltage and also it can be implemented digitally easier in comparison to other techniques. So DFIG using SVPWM topology is best suited for practical implementation. Using all the converter topologies dynamic response of DFIG for decoupled control of active and reactive powers has been presented.

APPENDIX

ω_e	Synchronous Speed	376 rad/s
L_m	Magnetizing inductance	0.0538 H
R_s	Stator Resistance	0.183 ohm
R_r	Rotor resistance	0.277 ohm
L_s	Stator inductance	0.0553 H
L_r	Rotor Inductance	0.056 H
P	No. Of Pole Pairs	2
J	Moment of Inertia	0.0165

REFERENCE

- Yu Zou, Malik Elbuluk and Yilmaz Sozer, "A Complete Modeling and Simulation of Induction Generator Wind Power Systems" IEEE 2010.
- T.Ghennam, E.M.Berkouk," Modeling and control of a Doubly Fed Induction Generator (DFIG) Based Wind Conversion System", IEEE March 18-20,2009, Laboratoire d' Elctronique de Pussance,Algeria.
- Dendouga , R. Abdessemed, M. L. Bendaas and A. Chaiba " Decoupled Active and Reactive Power Control of a Doubly-Fed Induction Generator (DFIG)''proceedings of the 15th Mediterranean conference on control & Automation, July27-29,2007 Athence-Greece.
- Muhammad H Rashid, Power Electronics Circuits, Devices and Applications, Prentice Hall of India Private Limited, New Delhi, 2004.
- Lingling Yan, Xianshan Li Hanwen Hu and Boya Zhang, "Research on SVPWM Inverter Technology in Wind Power Generation System' IEEE 2011.
- H. Karimi-Davijani, R.Ahmadi, H.Livani, "Active and Reactive Power Control of DFIG Using SVPWM Converter" IEEE.
- D. Grahame Holmes, Thomas A.Lipo, "Pulse Width Modulation for Power Converters, Principles and practice" IEEE Press, WILEY publication.

K.H.Phani shree received B.Tech degree from Bapatla Engineering College, bapatla in the year 2000. She received the M.E. degree in power systems from NIT Trichy, Tamil Nadu In 2002.currently she is assistant professor at Jawaharlal Nehru Technological University, Hyderabad. Her research interests include Power Electronics, FACTS and Renewable energy sources'.

Dr. S. V. Jayaram Kumar received the M.E. degree in electrical engineering from the Andhra University, Vishakhapatnam, India, in 1979.He received the Ph.D. degree in electrical engineering from the Indian Institute of Technology, Kanpur, in 2000. Recipient of President of Indian Medal for Best Paper among all Engineering disciplines constituted by Institution of Engineering India in the year 2000.Currently, he is a professor at Jawaharlal Nehru Technological University, Hyderabad. His research interests include Power Electronics, FACTS and Power systems.